Original Article

Institution of MECHANICAL ENGINEERS

Journal of RAIL AND RAPID TRANSIT

Proc IMechE Part F:
J Rail and Rapid Transit
0(0) 1–12

DOI: 10.1177/0954409718773014
journals.sagepub.com/home/pif

SAGE

Analysis of vertical vibration characteristics of the vehicle-flexible track coupling system under wind load and track irregularity

Zhanling Ji, Guowei Yang, Yubiao Liu and Qian Jiang

Abstract

In this study, to overcome the inherent problem caused by simulating infinite rail using finite rail, a method that combines flexible rail embedded in SIMPACK and a flexible track board imported from ANSYS on a SIMPACK platform is first proposed, by which vehicle-flexible track coupling is effectively realized. The method takes into account the simulation precision and computational efficiency. Using the proposed method, and comprehensively considering wind load, track irregularity, and minor track elasticity, the dynamic characteristics of high-speed train are solved conveniently and quickly. They are simulated under the conditions close to the objective reality. On this basis, the influences of many factors on the vibration characteristics of the train are analyzed, which include car body state, track state, mode numbers of the car body, wind load, track irregularity, and vehicle speed. In addition, the simulation results are basically consistent with the test results. This work lays a solid foundation for subsequent research on noise, fatigue, and the reliability of the train.

Keywords

High-speed train, vibration characteristics, multi-level rigid-flexible coupling, vehicle-flexible track coupling

Date received: 28 March 2017; accepted: 30 March 2018

Introduction

Railways are known to be an important national infrastructure, economic artery, and popular traffic tool. It is also the backbone of the transportation system. With the sustainable development of the world economy and industries, railway transport is required to gradually develop towards attaining high speed, heavy load, and comfort. However, with the increase in the train speed, the dynamic actions of the air around the train and the influence of track irregularity become more pronounced. The violent wheel–rail action force also exacerbates the deformation and subsidence of the track. More exacerbated action and vibration are transferred to car body thereby seriously affecting the ride comfort. Owing to the long-term vibrations, fatigue damage occurs in the weaker parts of trains, which causes a decrease in the structural reliability, shortens service life, and even threatens the driving safety.

In addition, flexible track can reflect minor displacement caused by the vibration and vehicle gravity; thus, the results of analysis are in better accordance with the objective reality. Therefore, with respect to wind load and track irregularity considering the vehicle-flexible track coupling, research on the vibration characteristics on high-speed train has become an important issue in terms of railway transportation.

For a long time, a lot of theoretical analyses, simulations, and experimental researches have been carried out with regard to the vibration of high-speed train. With respect to vehicle-flexible track coupling, remarkable achievements and progress have been also made. Liu et al.[1] realized the coupling of vehicle and track systems by vertical wheel–rail contact force, which was determined by the use of simplified nonlinear Hertzian contact theory. Aceituno et al.[2] adopted the finite element floating frame of reference approach and modal reduction techniques for rail flexibility. Under dynamic loading conditions, using

Institute of Mechanics, Chinese Academy of Sciences, Beijing, China

Corresponding author:
Guowei Yang, Institute of Mechanics, Chinese Academy of Sciences, Beijing 100190, China.
Email: gwyang@imech.ac.cn

a self-developed multi-body system (MBS) code, El-Ghandour et al.[3] analyzed the deformation of flexible track and substructure by Hertzian contact, and creepages as defined by Kalker. Using the moving Green function, Sheng et al.[4] dealt with interactions between wheels and a track with or without rail dampers. Through moving element method, Dai et al.[5] studied a high-speed track system that was discretely supported. To understand the vehicle–structure interaction, the direct method was used to formulate governing equilibrium equations and impose constraint equations.[6] To extend the range of validity above 1.5 kHz, a 3D track model based on moving element method was developed by adopting cyclic boundary conditions and Eulerian coordinates to replace the Timoshenko beam.[7] Dynamic contact forces between moving vehicles and rails were considered as internal forces, and thus, the excitation vectors of load between wheels and rails, induced by a vehicle's weight and random track irregularities, were easily formulated using the pseudo-excitation method.[8] The wheel–rail interaction forces were determined by Kalker's creep theory and Hertz's contact theory.[9] Train and track were interconnected by Hertzian springs and modeled as a coupled system.[10] Ling et al.[11] calculated the normal wheel–rail force using the nonlinear Hertzian contact spring model, and the creep force was determined using Shen et al.'s (1983) model based on Kalker's (1967) linear creep theory. In the literature mentioned above, the wheel–rail interaction was mostly achieved by self-developed programs. The kind of method adopted was flexible and controllable, but it had high requirements for the users. Li et al.[12–14] conducted the vibration analysis of vehicle–bridge coupling by ANSYS and SIMPACK, in which the vehicle–bridge coupling was realized through data exchange at discrete information points of the wheel–rail contact surface. But rails together with bridge are seen as flexible track. They are different from the rails treated as flexible track, and fastener, track board and cement asphalt (CA) mortar also considered. Chen[15] applied dummy elements to interconnect wheel and rail, but constraint type at both ends of the finite rail had a significant influence on the vibration characteristics, and the preprocessing was found to be complex.

From the above discussion, it is clear that a method that takes into account the simulation precision and computational efficiency, is user-friendly, and is suitable for the vast majority of the users is crucial to be proposed. Therefore, by integrating more powerful SIMPACK software for modeling wheel–rail contact and more efficient ANSYS software for modeling flexible parts, a discrete node method is presented to realize the vehicle–flexible track interaction. Based on the proposed method, the research on the vibration characteristics of a high-speed train is developed.

Problem formulation and mathematical model

The coupling system of high-speed train experiences aerodynamic effect caused by strong airflow and ambient wind, and the wheel–rail interaction exacerbated by track irregularity. The motion posture change of the vehicle and the deformation of car body are induced by strong airflow and ambient wind. The vibration is induced by track irregularity and track elasticity, which travels through the vehicle by the wheel–rail contact. Therefore, in the study of the vibration problem of high-speed train, the aerodynamic effect, track irregularity, and track elasticity should be comprehensively considered.

Vehicle model

In the vehicle model, all of bogie frame, wheelset, and axle box are treated as rigid bodies. Five degrees of freedom such as lateral, vertical, roll, pitch, and yaw are considered in a bogie frame or wheelset. One pitch degree of freedom is considered in an axle box. Car body is flexible.

The differential vibration equation of the vehicle system is as follows

$$[M]\{u\} + [C]\{u\} + [K]\{u\} = \{Q\} \tag{1}$$

where $[M]$ is the mass matrix, $[C]$ is the damping matrix, $[K]$ is the stiffness matrix, $\{u\}$ is the displacement vector, $\{Q\}$ is the dynamic load induced by vehicle gravity, track irregularity, and wind load.

When the car body is flexible, its displacement calculation is conducted by the following mode superposition method

$$\{u(t)\} = \sum_{i=1}^{m} \xi_i(t)\{\phi_i\} = [\Phi]\{\xi(t)\} \tag{2}$$

where $[\Phi]$ is the modal vector matrix, $\{\xi(t)\}$ is the generalized displacement vector, and m is the intercepted mode numbers of car body.

Rail model

A rail is treated as a Timoshenko beam with elastic discrete supports. The differential equation of its vertical vibration is as follows

$$\rho_{\mathrm{r}} A_{\mathrm{r}} \frac{\partial^2 Z_{\mathrm{r}}(x,t)}{\partial t^2} + k_{\mathrm{r}z} G_{\mathrm{r}} A_{\mathrm{r}} \left(\frac{\partial \phi_{\mathrm{r}}(x,t)}{\partial x} - \frac{\partial^2 Z_{\mathrm{r}}(x,t)}{\partial x^2} \right) = -\sum_{i=1}^{N_{\mathrm{s}}} F_{\mathrm{rs}i}(t)\delta(x - x_{\mathrm{rs}i}) + \sum_{j=1}^{N_{\mathrm{w}}} p_j \delta(x - x_{\mathrm{w}j})$$

$$\rho_{\mathrm{r}} I_{\mathrm{r}y} \frac{\partial^2 \phi_{\mathrm{r}}(x,t)}{\partial t^2} - E_{\mathrm{r}} I_{\mathrm{r}y} \frac{\partial^2 \phi_{\mathrm{r}}(x,t)}{\partial x^2}$$

$$+k_{rz}G_rA_r\left(\phi_r(x,t)-\frac{\partial Z_r(x,t)}{\partial x}\right)=0 \tag{3}$$

where ρ_r is the density of the rail, $Z_r(x,t)$ is the vertical displacement of the rail, E_r is the elastic modulus of the rail, I_{ry} is the rotary inertia of the rail cross section about y-axis, A_r is the cross-sectional area of the rail, ϕ_r is the rotation angle of the rail section about y-axis, k_{rz} is the shear factor, G_r is the shear modulus of the rail, $F_{rsi}(t)$ is the fastener force acting on the rail, p_j is the wheel–rail force, δ is the impact function, i is the fastener numbers, j is the wheelset numbers, x_{rs} are the position coordinates of the fasteners, x_w are the position coordinates of the wheelset, N_s are fastener numbers, and N_w are the wheelset numbers.

Based on the mode superposition method, vertical displacement and rotation angle about y-axis of the rail can be expressed as

$$\begin{aligned} Z_r(x,t)&=\sum_{k=1}^{N_V}Z_k(x)q_{zk}(t)\\ \phi_r(x,t)&=\sum_{k=1}^{N_V}\phi_{rk}(x)w_{zk}(t)\end{aligned} \tag{4}$$

where N_V is the intercepted mode numbers of the rail, $Z_k(x)$ is the vertical regular mode function, q_{zk} is the vertical regular mode coordinates, $\phi_{rk}(x)$ is the regular mode function of rotation angle, and $w_{zk}(t)$ is the regular mode coordinates of the rotation angle with vertical vibration.

The regular mode functions of a Timoshenko beam simply supported at both ends are as follows

$$\begin{aligned} Z_k(x)&=\sqrt{\frac{2}{m_rl}}\sin\left(\frac{k\pi x}{l}\right)\\ \phi_{rk}(x)&=\sqrt{\frac{2}{\rho_rI_{ry}l}}\cos\left(\frac{k\pi x}{l}\right)\end{aligned} \tag{5}$$

where l is the length of the rail, and m_r is the mass per unit length of the rail.

According to the nature of δ function and orthogonality of the mode, the second-order ordinary differential equation with regard to the mode coordinates is as follows

$$\begin{aligned} &\ddot{q}_{zk}(t)+\frac{k_{rz}G_rA_r}{m_r}\left(\frac{k\pi}{l}\right)^2q_{zk}(t)\\ &\quad-k_{rz}G_rA_r\frac{k\pi}{l}\sqrt{\frac{1}{m_r\rho_rI_{ry}}}w_{zk}(t)\\ &=-\sum_{i=1}^{N}F_{rsi}Z_k(x_{rsi})+\sum_{j=1}^{4}P_jZ_k(x_{wj})\end{aligned}$$

$$\begin{aligned} &w_{zk}(t)+\left(\frac{k_{rz}G_rA_r}{\rho_rI_{ry}}+\frac{E_rI_{ry}}{\rho_rI_{ry}}\left(\frac{k\pi}{l}\right)^2\right)w_{zk}(t)\\ &\quad-k_{rz}G_rA_r\frac{k\pi}{l}\sqrt{\frac{1}{m_r\rho_rI_{ry}}}q_{zk}(t)=0\end{aligned} \tag{6}$$

Track board model

In the vertical direction, track board can be simplified as an elastic plate. According to the elastic thin plate theory, differential equation of its vertical vibration can be written as

$$\begin{aligned} &\frac{\partial^4\omega(x,y,t)}{\partial x^4}+2\frac{\partial^4\omega(x,y,t)}{\partial x^2\partial y^2}+\frac{\partial^4\omega(x,y,t)}{\partial y^4}\\ &\quad+\frac{C_s}{D_s}\frac{\partial\omega(x,y,t)}{\partial t}+\frac{\rho_sh_s}{D_s}\frac{\partial^2\omega(x,y,t)}{\partial t^2}\\ &=\frac{1}{D_s}\left[\sum_{i=1}^{N_p}P_{rVi}(t)\delta(x-x_{pi})\delta(y-y_{pi})\right.\\ &\quad\left.-\sum_{j=1}^{N_b}F_{sVj}(t)\delta(x-x_{bj})\delta(y-y_{bj})\right]\end{aligned} \tag{7}$$

where N_p are fastener numbers on a track board, N_b are support numbers under a track board, $\omega(x,y,t)$ is the vibration deflection of a track board, x_{pi} and y_{pi} are the longitudinal and lateral locations of the ith fasteners, respectively, x_{bj} and y_{bj} are the longitudinal and lateral locations of the jth support, respectively, ρ_s is the density of a track board, C_s is the damping of a track board, D_s is the bending stiffness, P_{rVi} is the vertical force of the ith fasteners, and F_{sVj} is the vertical reaction force of the jth support.

The deflection solution of a track board can be written as

$$\omega(x,y,t)=\sum_{m=1}^{N_x}\sum_{n=1}^{N_y}X_m(x)Y_n(y)T_{mn}(t) \tag{8}$$

where N_x and N_y are the intercepted mode numbers in the directions of length and width of a track board, $X_m(x)$ and $Y_n(y)$ are the vibration mode functions in the directions of length and width of a track board, respectively, and $T_{mn}(t)$ is the normal coordinate of a track board.

The second-order ordinary differential equation of the vertical vibration of a track board regarding the normal coordinates can be written as

$$\begin{aligned} &\ddot{T}_{mn}(t)+\frac{c_s}{\rho_sh_s}\dot{T}_{mn}(t)+\frac{D_s}{\rho_sh_s}\frac{B_3B_2+2B_4B_5+B_1B_6}{B_1B_2}T_{mn}(t)\\ &=\frac{1}{\rho_sh_sB_1B_2}\left[\sum_{i=1}^{N_p}P_{rVi}(t)X_m(x_{pi})Y_n(y_{pi})\right.\end{aligned}$$

$$-\sum_{j=1}^{N_b} F_{svj}(t) X_m(x_{bj}) Y_n(y_{bj}) \Big] \quad (9)$$

where $B_1 = \int_0^{L_s} X_m^2(x)\mathrm{d}x$, $B_2 = \int_0^{W_s} Y_n^2(y)\mathrm{d}y$, $B_3 = \int_0^{L_s} X_m'''(x)X_m(x)\mathrm{d}x$, $B_4 = \int_0^{L_s} X_m''(x)X_m(x)\mathrm{d}x$, $B_5 = \int_0^{W_s} Y_n''(y)Y_n(y)\mathrm{d}y$, $B_6 = \int_0^{W_s} Y_n'''(y)Y_n(y)\mathrm{d}y$.

Vehicle–track coupling dynamics model of a high-speed train

Multi-level rigid-flexible coupling dynamics model

Within the framework of multi-body systems, for simulating the movement behavior of a high-speed train on a long line, the vehicle-flexible track coupling is a core problem to study the vibrational characteristics of a train. Under the premise of ensuring calculation accuracy, it is of great engineering value and practical significance to establish a reasonably simplified vehicle–track interface coupling model.

Presently, some researchers[15] have achieved the vehicle-flexible track coupling through dummy method. Its principle is shown in Figure 1, where the wheel–rail contact force and displacement are transmitted by constraints, force elements, and dummy elements. The mass and rotary inertia of each dummy element are very small, which is used to connect a moving rigid rail with a fixed flexible rail. However, all the above elements are defined in the preprocessing, and so the preprocessing workload is large. And the influence of constraint type at both ends of a rail on calculation results is larger, thereby the potential inherent problem simulating infinite rail using finite rail cannot be avoided.

Elaborating on the influence, the entire track is regarded as a separate system. In the light of track parameters, when the track is long enough, that is to say the constraint influence at both ends of the track is very small, vertical force of each fastener is 382 N, and vertical force at each node of CA mortar is 4412 N. Fasteners are expressed by spring-damper force elements, which are imposed on two markers, where positive forces try to pull the markers up to each other and negative forces try to push them away. Using the dummy method, when both ends of the rail are free or connected with track board by force elements, by the preload calculation in SIMPACK, it is found that the vertical forces of the fasteners are 350–435 N, and those at the nodes of CA mortar are 4350–4500 N. Whereas when both ends of the rail are fixed at the ground, by the preload calculation in SIMPACK, the vertical forces of the fasteners are −2300 to −1500 N, and those the nodes of CA mortar are from 1700 to 2500 N. By comparative studies, when both ends of the rail are free or connected with track board by the force elements, all the forces are basically normal. However, when both ends of the rail are fixed at the ground and middle part of the rail is supported by some fasteners, due to rail with redundant constraints, finite rail length, large stiffness, small mass, and so on, the vertical forces of the fasteners are negative, which shows that the springs representing the fasteners are tensioned, and the vertical forces of CA mortar are also greatly reduced. These facts manifest that part of the rail gravity is passed on to the ground by the fixed constraints when both ends of the rail are fixed at the ground, which leads to the decrease of the vertical downward displacements for both rail and track board. At the time, even if the train is placed on the track, the vertical downward displacements of the track still decrease. In addition, if both ends of the rail are free or connected with the track board by the force elements, because flexible rails, flexible track boards, dummy elements, spring-damper force elements, and constraints are introduced, solving efficiency is greatly reduced. Moreover, when length of the rail is shorter, upwarping or sinking phenomenon at both ends is obvious, and thus the solution results are far away from that of a long rail. If the rail is prolonged, modeling and solving efficiencies are found to be very low. Compared to track irregularity, the displacement caused by flexible track is much smaller. However, it significantly influences the vibration characteristics of the train. To reflect the real situation as much as possible, flexible track should be better simulated.

To address the problems that exist in the above method, a method that combines flexible rail embedded in SIMPACK and a flexible track board

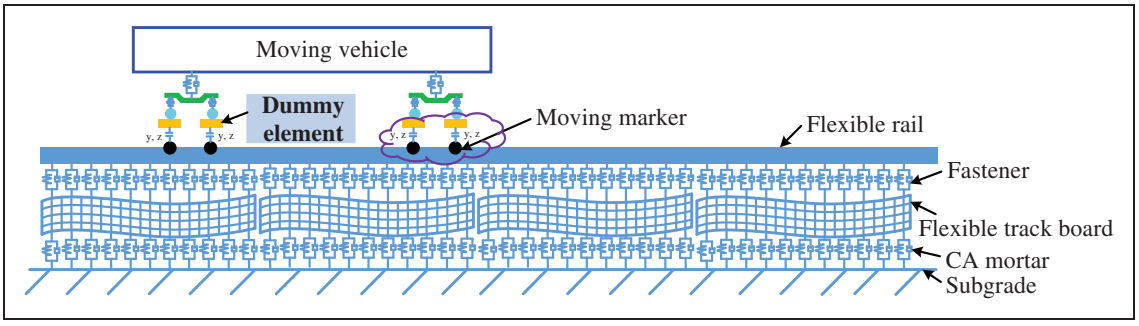

Figure 1. Vehicle-flexible track coupling principle by dummy elements.

imported from ANSYS is put forward. Its principle is shown in Figure 2. The vehicle locations running on flexible track are identified by wheel–rail contact discrete nodes, which are established through flexible track configuration file. Thereby the displacement, velocity, and force between wheels and rails are exchanged. The interactions are achieved by spring-damper force elements between rails and track boards, and track boards and the subgrade. The function of flexible track is directly embedded in the SIMPACK program. For the rail, modeling and coupling with vehicle are easy. All the dummy elements, force elements, and constraints introduced between rigid rails and flexible rails are eliminated. The solution efficiency is higher. For example, at a train speed of 400 km/h and 169 m track length, considering the wind load, track irregularity and track elasticity, flexible car body, and free constraint at both ends of the rail, it is seen that the solution time of the discrete node method is 8 h and 6 min, which is closely related to the hardware configuration and the current utilization of CPU, whereas that of the dummy element method is about five days. As a result of using discrete rail nodes to transfer data, the influence of constraint type at both ends of finite rail is reduced.

In Figure 3, the calculation results are shown for the cases that dummy element method is used and both ends of the rail are fixed, and discrete node method is used and both ends of the rail is freely supported; here both track irregularity and wind load are not considered. In comparison to the proposed method, when dummy method is used, both vertical displacement of a wheelset and vertical force of a fastener are much smaller. Based on the multi-rigid-body model of the train, considering the flexibility of the car body, rail, and track board and applying discrete node method to the wheel–rail contact, the flexible car body–flexible rail–flexible track board–subgrade coupling dynamics model is established in Figure 4.

Vehicle-flexible track coupling flow

Figure 5 shows the vehicle-flexible track coupling flowchart by using the proposed method. Firstly, for car body, rail, and track board, flexibility treatments

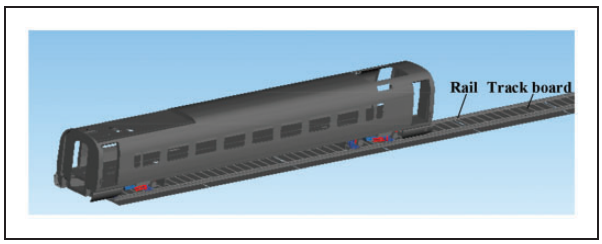

Figure 4. The flexible car body–flexible rail–flexible track board–subgrade coupling dynamics model of a high-speed train.

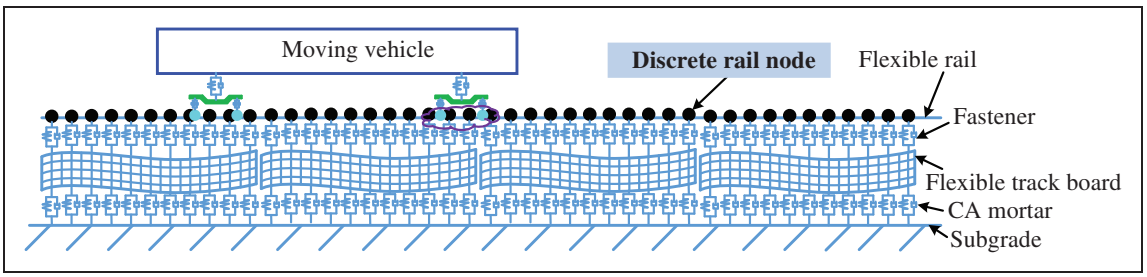

Figure 2. Vehicle-flexible track coupling principle by discrete rail nodes.

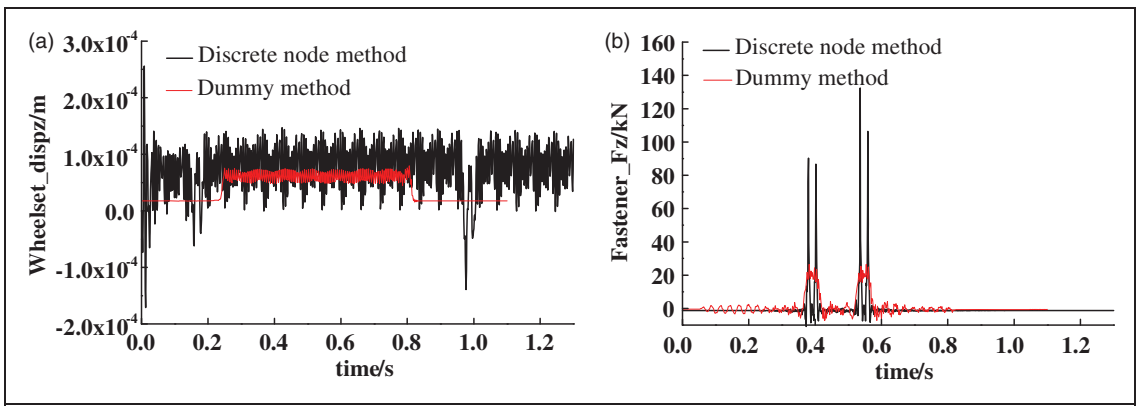

Figure 3. Vibration characteristics of the train using two methods: (a) vertical displacement of a wheelset and (b) vertical force of a fastener.

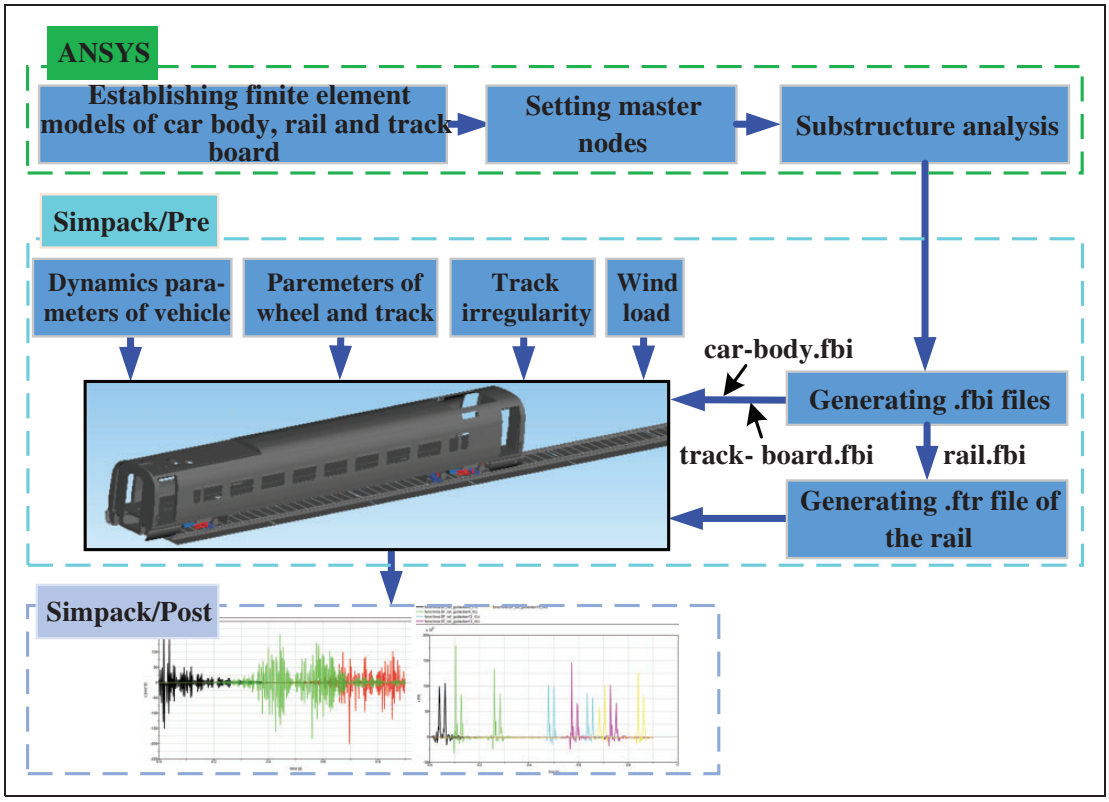

Figure 5. Flowchart of vehicle-flexible track coupling by discrete node method for the rail.

in ANSYS and flexible body files (.fbi files) generated in SIMPACK are carried out. Then, for car body and track board, they are integrated into the dynamics model of high-speed train as flexible bodies, whereas for rail, its flexible rail configuration file (.ftr file) is needed to interconnect the wheel and the rail.

Research cases

To study the influence of different conditions on vibration characteristics of a high-speed train, the following basic conditions are considered: flexible car body with the first 30 elastic modes, flexible rail, flexible track board, track irregularity, and cross wind, with a running speed of 400 km/h. The conditions for the other cases studied are as follows: rigid car body, flexible car body with the first 10, 20, 40, and 45 elastic modes, regardless of the track irregularity and cross wind, with running speeds of 350 km/h, 380 km/h, and 415 km/h, and rigid track. The cross-wind speed is 15 m/s, and wind loads at a certain vehicle speed are constant (see Figure 6). When the calculation of aerodynamics is carried out for the train under a certain wind velocity, wind forces and wind torques around its mass center and output for the car body are calculated. When the dynamic analysis is carried out, they are treated as excitations and imposed at the mass center of the car body, where the mass center is a concentration point. The main parameters are listed in Table 1 by taking a CRH3 type of train as an example.

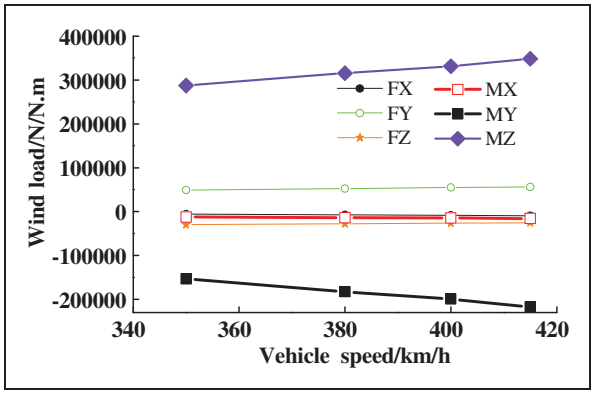

Figure 6. Wind load at different vehicle speeds.

Results and discussion

Different car body and track states

Four cases are studied, namely the rigid car body–rigid track, rigid car body–flexible track, flexible car body–rigid track, and flexible car body–flexible track. Flexible track is a group of flexible rails, fastener spring-damper force elements, flexible track board, CA mortar spring-damper force elements, and subgrade. Rigid track is a group of rigid rail and rigid

Table 1. Main parameters of the CRH3 type of train.

Parameter	Value
Distance between bogie centers of one unit	17.375 m
Wheelbase	2.5 m
Lateral span of wheel rolling circle	1.493 m
Diameter of wheel rolling circle	0.92 m
Distance between backs of the wheel flanges	1.353 m
Wheel profile	S1002G
Rail mass per unit length	60 kg/m
Mass of car body	38,884 kg
Roll inertia of car body	1,259,000 N·m^2
Pitch inertia of car body	19,053,000 N·m^2
Yaw inertia of car body	17,979,000 N·m^2
Height of gravity center of car body	1.656 m
Longitudinal stiffness of a primary spring	919,800 N/m
Lateral stiffness of a primary spring	919,800 N/m
Vertical stiffness of a primary spring	886,005 N/m
Damping of a primary vertical damper	10,000 N·s/m
Joint stiffness of a primary vertical damper	7,500,000 N/m
Longitudinal stiffness of an axle box rotary arm joint	120,000,000 N/m
Lateral stiffness of an axle box rotary arm joint	12,500,000 N/m
Damping of an anti-yaw damper	225,000 N·s/m
Joint stiffness of an anti-yaw damper	35,000,000 N/m
Longitudinal stiffness of a secondary air spring	133,000 N/m
Lateral stiffness of a secondary air spring	133,000 N/m
Vertical stiffness of a secondary air spring	203,000 N/m
Damping of a secondary vertical damper	10,000 N·s/m
Joint stiffness of a secondary vertical damper	5,000,000 N/m
Damping of a secondary lateral damper	15,000 N·s/m
Joint stiffness of a secondary lateral damper	4,250,000 N/m
Free clearance of a lateral stop	0.02 m
Roll angle stiffness of the anti-roll rod	4,150,000 N·m/rad

support. Both wind load and track irregularity are considered. Vehicle speed is 400 km/h and the first 30 elastic modes are intercepted for flexible car body. The results are shown in Figure 7.

By analyzing Figure 7, the following main conclusions are drawn:

1. The influence of the case "flex car body + rigid track" on the vibration characteristics of a high-speed train is remarkable, which even exceeds the case "flex car body + flex track" sometimes.
2. On the whole, the vibration characteristics of the car body are greatly influenced by the car body state. For example, at 0.039 s, the vertical displacement of the car body under the case "flexible car body + flexible track" is 26.8 mm larger than that under the case "rigid car body + flexible track." The vertical displacement of the car body under the case "flexible car body + rigid track" is 30.9 mm larger than that under the case "rigid car body + rigid track." Similarly, there are also vertical acceleration of the car body, and PSD of the vertical acceleration of the car body.
3. The track state has a significant influence on the vibration characteristics of the wheelset. For example, at 0.625 s, the vertical displacement of the wheelset under the case "rigid car body + flexible track" is 2.15 mm larger than that under the case "rigid car body + rigid track," and corresponds to 142.38%. The vertical displacement of the wheelset under the case "flex car body + flexible track" is 2.62 mm larger than that under the case "flex car body + rigid track," and corresponds to 256.86%. Similarly, there are also vertical acceleration of the wheelset at 0.362 s, and PSD of the vertical acceleration of the wheelset is 171.2 Hz.
4. The vibration characteristics of bogie frame are affected by both the car body state and track state. For example, at 0.8 s, the vertical acceleration of the bogie frame under the case "rigid car body + flexible track" is 1.68 m/s^2 larger than that under the case "rigid car body + rigid track," and corresponds to 192.16%. The vertical acceleration of the bogie frame under the case "flexible car body + flexible track" is 2.38 m/s^2 larger than that under the case "flexible car body + rigid track," and corresponds to 340.82%. The vertical acceleration of bogie frame under the case "flexible car body + flexible track" is 2.2056 m/s^2 larger than that under the case "rigid car body + flexible track," and corresponds to 252.64%. The vertical acceleration of the bogie frame under the case "rigid car body + rigid track" is 1.85 m/s^2 larger than that under the case "flexible car body + rigid track," and corresponds to 265.27%.
5. From the PSD curves of the vertical acceleration, when the track is flexible, higher frequency vibration exists in the wheelset and bogie frame, such as 171.2 Hz. However, it does not exist in the car body due to vibration isolation and vibration weakening of the primary and second spring dampers. These indicate that when the train speed is higher, the influence of each factor is more significant, and under the combined influence of various factors, higher vibration frequency of the flexible track is excited, the resonance phenomenon occurs in the vehicle-flexible track coupling system, which significantly influences the vibration characteristics of the bogie frame and wheelset.

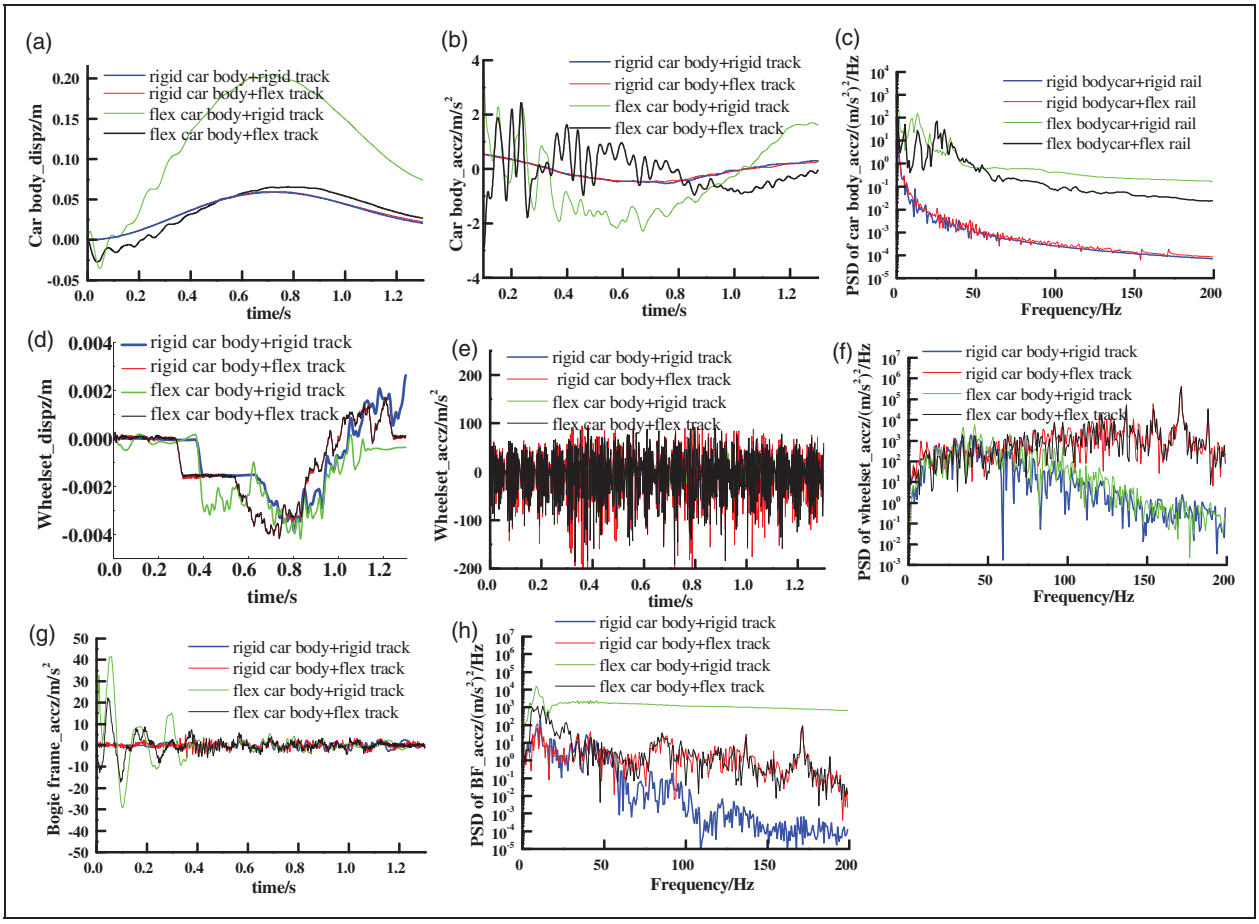

Figure 7. Vibration characteristics of the train under different car body and track states: (a) vertical car body displacement, (b) vertical car body acceleration, (c) power spectral density (PSD) of vertical car body acceleration, (d) vertical wheelset displacement, (e) vertical wheelset acceleration, (f) PSD of vertical wheelset acceleration, (g) vertical bogie frame acceleration, and (h) PSD of vertical bogie frame acceleration.

6. The vertical vibration acceleration of the wheelset is much larger than that of the bogie frame and car body. For example, the maximum vertical vibration acceleration of the wheelset, bogie frame, and car body are 200 m/s^2, 41.55 m/s^2, and 4 m/s^2, respectively. It shows isolation and weakening validities of the primary and secondary suspensions.

Different car body mode numbers

When the car bodies with the first 10, 20, 30, 40, and 45 elastic modes are used, respectively, the vibration characteristics of the train are as shown in Figure 8. At the time, both track elasticity and track irregularity are considered, and the vehicle speed is 400 km/h.

By analyzing Figure 8, the following main conclusions are obtained:

1. When the car body mode numbers intercepted is greater than 30, the vibration characteristics of the train basically remain unchanged. The vibration characteristics under the case "20 modes" are close to that under the case "30 modes." Besides the vertical displacement and acceleration of the wheelset, vibration characteristics under the case "10 modes" are far from that under the case "30 modes." For example, at 0.6 s, when the car bodies with the first 10, 20, 30, 40, and 45 elastic modes are used, the vertical displacements of the car body are 0.0094 mm, 26.83 mm, 27.41 mm, 27.41 mm, and 27.41 mm, respectively, which are 0.0343%, 97.88%, 100%, 100%, and 100% of that under the case "30 modes." Therefore, in the researches on the vibration characteristics, taking into consideration both the simulation precision and computational efficiency, the first 30 elastic modes intercepted are recommended for the flexible car body.
2. The mode numbers of the car body have significant influence on the vibration characteristics of the car body. For example, at 0.4 s, the vertical accelerations of the car body, bogie frame, and wheelset under the case "10 modes" are 0.45%, 39.5%, and 103.4% of that under the case "30 modes," respectively.

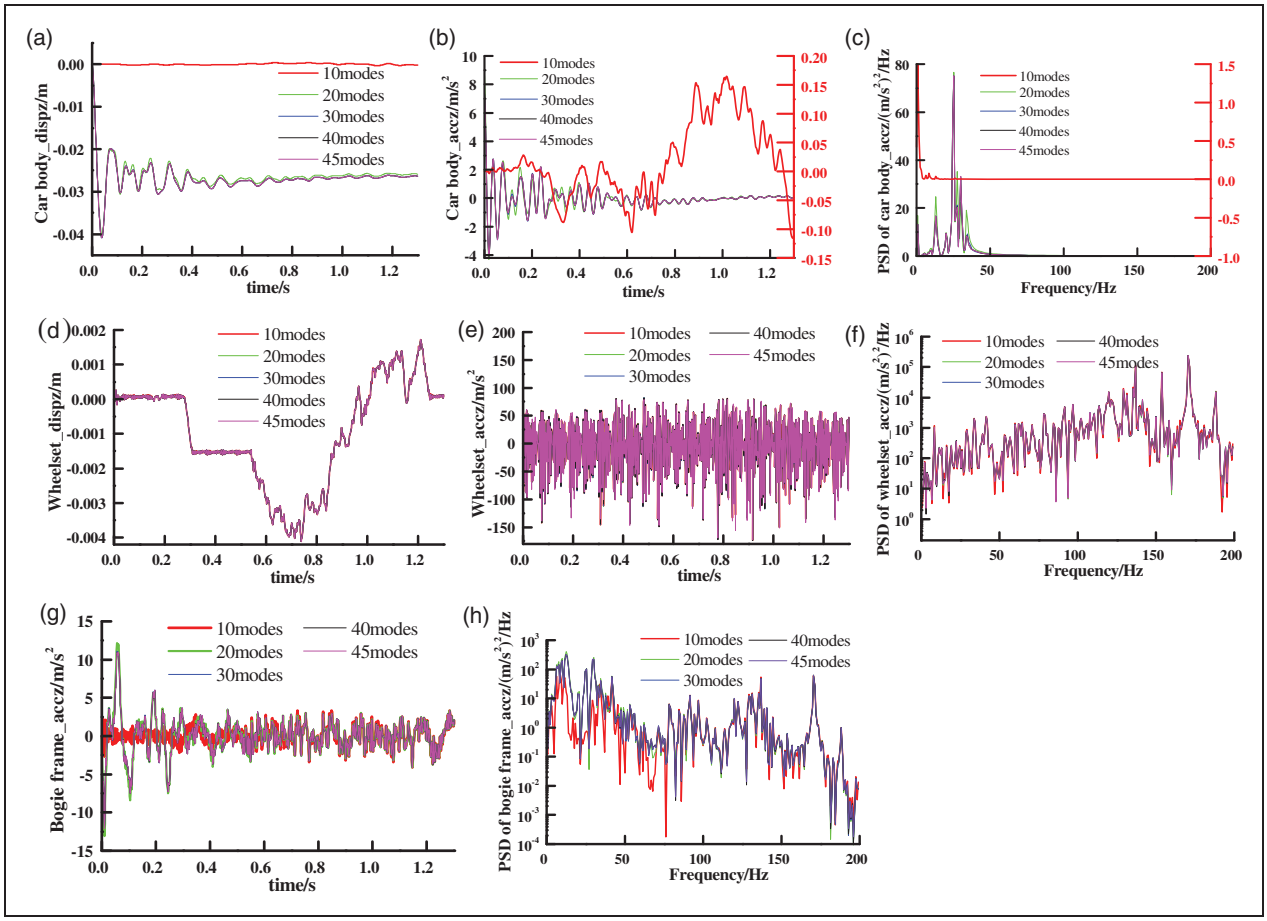

Figure 8. Vibration characteristics of the train under different car body mode numbers: (a) vertical car body displacement; (b) vertical car body acceleration (right vertical axis represents the acceleration of the car body under the case "10 modes"); (c) PSD of vertical car body acceleration (right vertical axis represents PSD of the car body acceleration under the case "10 modes"); (d) vertical wheelset displacement; (e) vertical wheelset acceleration; (f) PSD of vertical wheelset acceleration; (g) vertical bogie frame acceleration; and (h) PSD of vertical bogie frame acceleration.

Different running cases

Researches on the vibration characteristics of a high-speed train are carried out under the following three cases: considering track elasticity, track irregularity, and wind load. At the time, vehicle speed is 400 km/h, car body with the first 30 elastic modes are used, cross-wind speed is 15 m/s, running distance is 169 m, track irregularity is not considered within 30 m from both ends of the track. Their results are shown in Figure 9.

By analyzing Figure 9, the following main conclusions are obtained.

1. Wind load has a significant influence on the vibration characteristics of the car body and the reasons being the wind load directly imposed on the car body and the large size of the car body. For example, at 0.6 s, the vertical displacement of the car body under the case "flexible track + PSD + wind" is 9.61 mm smaller than that under the case "flexible track + PSD," and corresponds to 28.45%. Whereas the vertical displacement of wheelset under the case "flexible track + PSD + wind" is 0.04 mm larger than that under the case "flexible track + PSD," and corresponds to 1.38%.
2. Track irregularity has a significant influence on the vibration characteristics of the wheelset and the reason being the track irregularity imposed on the track and the direct wheel–rail contact. For example, at 0.6 s, the vertical displacement of the car body under the case "flexible track + PSD" is 1.23 times as large as that under the case "flexible track." Whereas the vertical displacement of the wheelset under the case "flexible track + PSD" is 28.35 times as large as that under the case "flexible track."
3. From the vertical displacement of the wheelset, the displacement caused by track elasticity is 1 or 2 orders of magnitude smaller than that caused by track irregularity. For example, at 0.738 s, the vertical displacement of the wheelset under the case "flexible track + PSD" is −4.11 mm, whereas that under the case "flexible track" is 0.067 mm, and corresponds to 61.34 times. But the influence of track elasticity on the vibration characteristics of

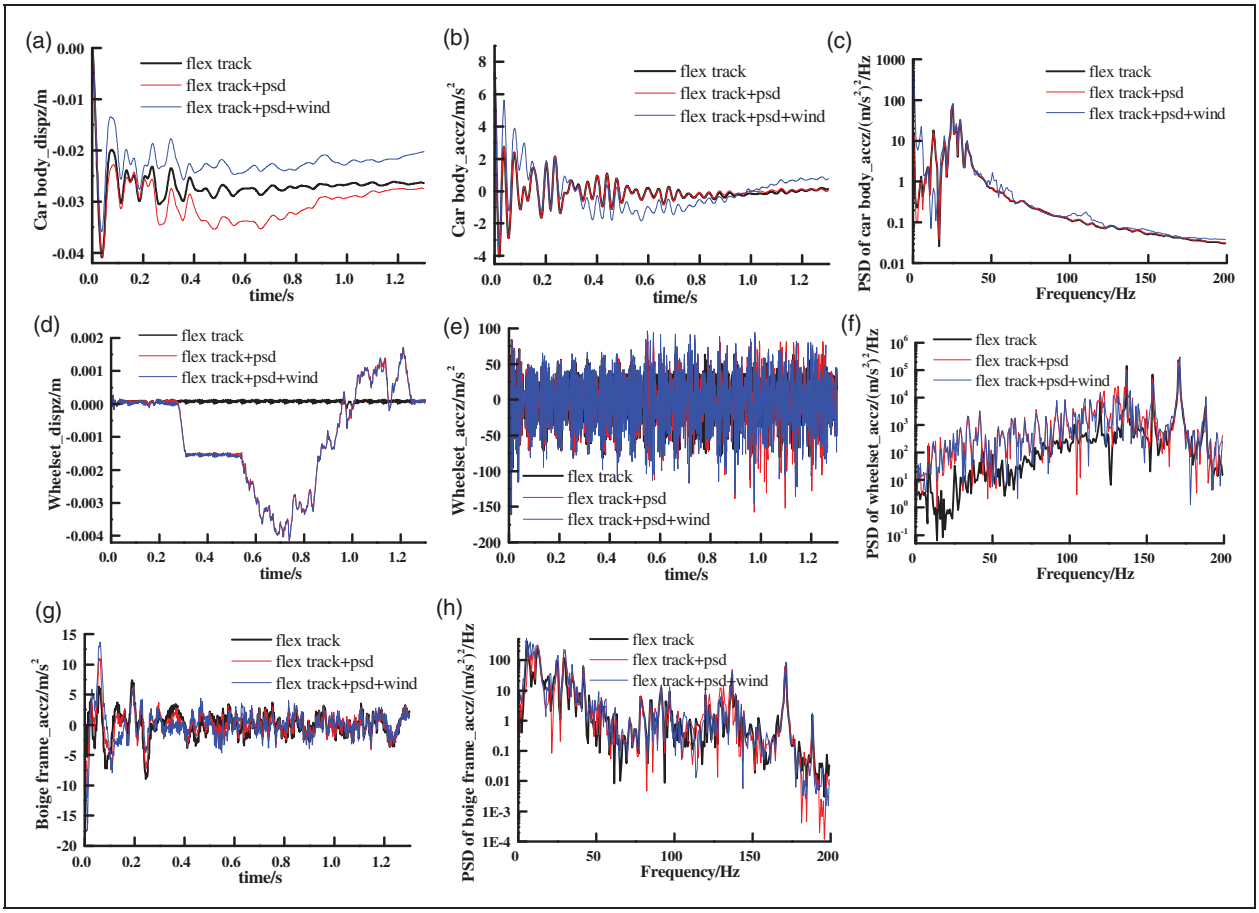

Figure 9. Vibration characteristics of the train under different cases: (a) vertical car body displacement; (b) vertical car body acceleration; (c) PSD of vertical car body acceleration; (d) vertical wheelset displacement; (e) vertical wheelset acceleration; (f) PSD of vertical wheelset acceleration; (g) vertical bogie frame acceleration; and (h) PSD of vertical bogie frame acceleration.

the train is non-negligible, as seen in the section of "Different car body and track states."

4. From the vertical displacement of the car body, wind load inhibits the vibration displacement of the car body to a certain extent. For example, at 0.624 s, the vertical displacement of the car body under the case "flexible track + PSD + wind" is −23.22 mm, whereas that under the case "flexible track + PSD" is −33.91 mm, and corresponds to 68.48%.

Different vehicle speeds

Figure 10 shows the vibration characteristics of the train when the vehicle speeds are 350 km/h, 380 km/h, 400 km/h, and 415 km/h, respectively. At the time, all of track elasticity, track irregularity, and wind load are considered, and the car body with the first 30 elastic modes is used. By analyzing it, the following conclusions are obtained.

1. With the increase in the running speed, the frequency corresponding to the peak vibration amplitude increases. Taking the frequency corresponding to the maximum vibration amplitude as an example, when vehicle speeds are 350 km/h, 380 km/h, 400 km/h, and 415 km/h, the frequencies are 150.6 Hz, 161.9 Hz, 171.2 Hz, and 177.9 Hz, respectively.
2. Owing to the comprehensive impact of multiple factors, at higher speed, the vibration amplitude is not necessarily higher. For example, at 100.6 Hz, when the vehicle speeds are 350 km/h, 380 km/h, 400 km/h, and 415 km/h, PSDs of the wheelset vertical acceleration are 1.34 $(m/s^2)^2/Hz$, 1.47$(m/s^2)^2/Hz$, 0.08$(m/s^2)^2/Hz$, and 5.59$(m/s^2)^2/Hz$, respectively.
3. From the vertical characteristics of the car body, at the middle and higher frequencies, such as 60–200 Hz, the increase in the running speed makes its vibration amplitude to slightly more fluctuate.

Validation

When the dynamics simulation for the train is carried out, it is imposed that the PSD of track

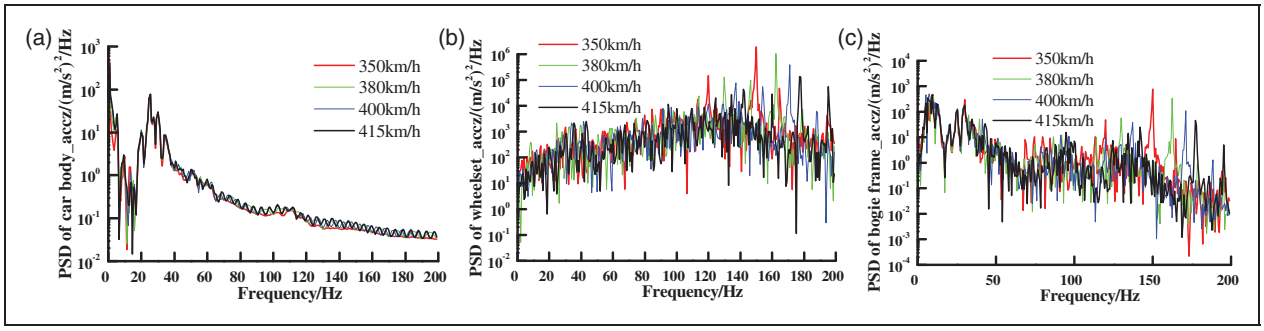

Figure 10. Vibration characteristics of the train under different train speeds: (a) PSD of vertical car body acceleration; (b) PSD of vertical wheelset acceleration; and (c) PSD of vertical bogie frame acceleration.

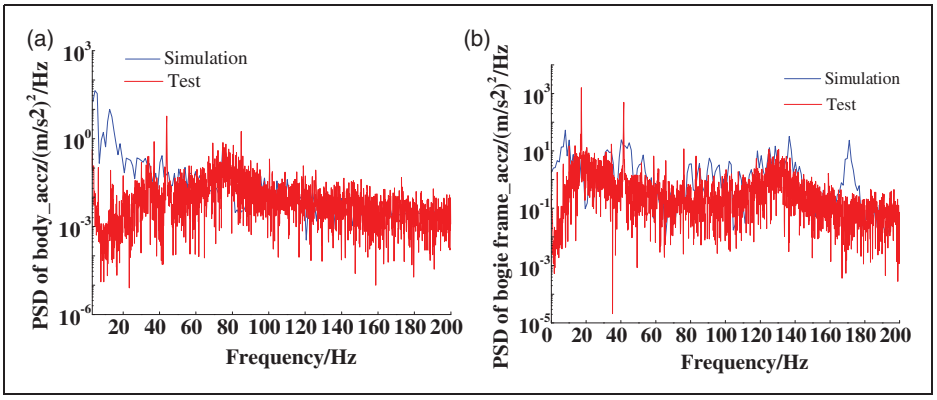

Figure 11. Vibration characteristics of the train under the simulation and test: (a) PSD of the vertical car body acceleration and (b) PSD of the vertical bogie frame acceleration.

irregularity of the high-speed railway from Beijing to Tianjin in China, and the running case is tri-car train and open air. Test results are the site tests from Beijing-Tianjin high-speed railway. When the test is conducted, the train is in the steady operation state, i.e. it does not include start acceleration and braking processes, and the rail is long enough. Figure 11(a) and (b) shows the PSD curves of the vertical acceleration of the car body and bogie frame, respectively. For comparison with the test results, when simulation results are plotted, the start acceleration stage is removed. From the figures, it is seen that two aspects of differences exist. One is the certain difference existing below 25 Hz, and the other is the frequencies and vibration amplitudes corresponding to several amplitude peak points. The reason being the simulation conditions are not completely the same with the test conditions, such as unidirectional aerodynamics/multi-body dynamics coupling and aerodynamics/multi-body dynamics interaction in the natural environment, and other disturbances. In the future work, dynamics simulation for the tight aerodynamics/multi-body dynamics coupling will be completed. On the whole, the simulation results are basically consistent with the test results.

Conclusions

Aimed at the influence of constraint type at both ends of finite rail on vibration characteristics, the method combining the flexible rail embedded in SIMPACK and the flexible track board imported from ANSYS is first put forward. Using the proposed method, by systematically considering the influences of the aerodynamic effect, track irregularity, wind load and track elasticity, the coupling of vehicle and flexible track is effectively realized, the exacerbated vibration problem induced by high speed can be conveniently and quickly solved, and working state of the train is truly reflected. By analyzing the calculation results, the following main conclusions are obtained:

1. The resonance phenomenon occurs in the vehicle-flexible track coupling system at higher frequencies. When the vehicle speed is 400 km/h, the frequency is 171.2 Hz.
2. When the vibration characteristics analysis for the train with flexible car body is carried out, the elastic mode numbers intercepted for the car body must be over 30.
3. Wind load has greater influence on the vibration characteristics of car body, whereas track

irregularity has greater influence on the vibration characteristics of the wheelset.
4. The vertical displacement of the wheelset caused by track elasticity is 1 or 2 orders of magnitude smaller than that caused by track irregularity, but the influence of track elasticity on the vibration characteristics of the train is non-negligible.
5. With the increase in the vehicle speed, the frequency corresponding to the maximum vibration amplitude increases, but vibration amplitude does not necessarily increase. When vehicle speeds are 350 km/h, 380 km/h, 400 km/h, and 415 km/h, the frequencies are found to be 150.6 Hz, 161.9 Hz, 171.2 Hz, and 177.9 Hz, respectively.
6. At 60–200 Hz, the increase in the running speed makes the vibration amplitude of the PSD of the vertical car body acceleration to slightly more fluctuate.

In further work, the interaction of the train and the air around it will be achieved. Its key technologies are data exchange and mesh deformation. Data exchange will be realized by RBF interpolation and virtual work principle. Mesh deformation will be realized by the combination of overset mesh and sticky mesh deformation.

Declaration of Conflicting Interests

The author(s) declared no potential conflicts of interest with respect to the research, authorship, and/or publication of this article.

Funding

The author(s) disclosed receipt of the following financial support for the research, authorship, and/or publication of this article: This study was supported by the National Key Research & Development Projects (Grant No.2017YFB0202801), the Strategic Priority Research Program of the Chinese Academy of Sciences (class B) (Grant No. XDB22020100), and Project funded by China Postdoctoral Science Foundation (Grant No. 2017M611010).

ORCID iD

Zhanling Ji http://orcid.org/0000-0003-1306-8285

References

1. Liu XY and Zhai WM. Analysis of vertical dynamic wheel/rail interaction caused by polygonal wheels on high-speed trains. *Wear* 2014; 314: 282–290.
2. Aceituno JF, Wang P, Wang L, et al. Influence of rail flexibility in a wheel/rail wear prediction model. *Proc IMechE, Part F: J Rail and Rapid Transit* 2017; 231: 57–74.
3. El-Ghandour AI, Hamper MB and Foster CD. Coupled finite element and multibody system dynamics modeling of a three-dimensional railroad system. *Proc IMechE, Part F: J Rail and Rapid Transit* 2016; 230: 283–294.
4. Sheng X, Xiao X and Zhang S. The time domain moving Green function of a railway track and its application to wheel–rail interactions. *J Sound Vib* 2016; 377: 133–154.
5. Dai J, Ang KK, Tran MT, et al. Moving element analysis of discretely supported high-speed rail systems. *Proc IMechE, Part F: J Rail and Rapid Transit* 2017; DOI: 0954409717693147.
6. Neves SGM, Montenegro PA, Azevedo AFM, et al. A direct method for analyzing the nonlinear vehicle–structure interaction. *Eng Struct* 2014; 69: 83–89.
7. Martínez-Casas J, Giner-Navarro J, Baeza L, et al. Improved railway wheelset–track interaction model in the high-frequency domain. *J Comput Appl Math* 2017; 309: 642–653.
8. Zeng ZP, Liu FS, Lou P, et al. Formulation of three-dimensional equations of motion for train–slab track–bridge interaction system and its application to random vibration analysis. *Appl Math Model* 2016; 40: 5891–5929.
9. Li YL, Xiang HY, Wang B, et al. Dynamic analysis of wind-vehicle-bridge coupling system during the meeting of two trains. *Adv Struct Eng* 2013; 16: 1663–1670.
10. Zhu ZH, Gong W and Wang LD. Hybrid solution for studying vibrations of coupled train–track–bridge system. *Adv Struct Eng* 2017; DOI: 10.1177/1369433217691775.
11. Ling L, Xiao XB, Xiong JY, et al. A 3D model for coupling dynamics analysis of high-speed train/track system. *J Zhejiang Univ-Sci A (Appl Phys & Eng)* 2014; 15: 964–983.
12. Li YL, Xu XY, Zhou Y, et al. An interactive method for the analysis of the simulation of vehicle–bridge coupling vibration using ANSYS and SIMPACK. *Proc IMechE, Part F: J Rail and Rapid Transit* 2016; DOI: 0954409716684277.
13. Han X, Zhu Bing, Wang JP, et al. Coupled vibration analysis of vehicle-bridge system for Jinsha River Bridge. *Appl Mech Mater* 2013; 361–363: 1194–1198.
14. Shan DS, Cui SA and Huang Z. Coupled vibration analysis of vehicle-bridge system based on multi-body dynamics. *J Transport Technol* 2013; 3: 1–6.
15. Chen M, Luo YY and Zhang B. Dynamic characteristic analysis of irregularity under turnout by vehicle-turnout rigid-flexible coupling model. *Adv Mater Res* 2014; 945–949: 591–595.